fire

MDPI

Article

Thermal Characteristics of Epoxy Fire-Retardant Coatings under Different Fire Regimes

Marina Gravit, Daria Shabunina * and Nikita Shcheglov

Peter the Great St. Petersburg Polytechnic University, Saint-Petersburg 195251, Russia; gravit_mv@spbstu.ru (M.G.); tsheglov.ne@edu.spbstu.ru (N.S.)
* Correspondence: shabunina.de@edu.spbstu.ru

Abstract: Different systems of fire protection coatings are used to protect the metal structures of stories and trestles at oil and gas facilities from low (when filling cryogenic liquids) and high temperatures (in case of the possible development of a hydrocarbon fire regime). This paper presents the results of experiments of fireproof coatings on an epoxy binder after the simulation of a liquefied hydrocarbons spill and subsequent development of a hydrocarbon fire regime at the object of protection and exposure of structures to a standard fire regime. According to the experimental results, the temperatures on the samples at the end of the cryogenic exposure were determined and the time from the beginning of the thermal exposure to the limit state of the samples at a hydrocarbon and standard temperature fire regime was determined. As a result, temperature–time curves in the hydrocarbon and standard fire regimes were obtained, showing good convergence with the simulation results. The solution of the inverse task of heat conduction using finite element modeling made it possible to determine the thermophysical properties of the formed foam coke at the end of the fire tests of steel structures with intumescent coatings. It was determined that an average of 12 mm of intumescent coating thickness is required to achieve a fire protection efficiency of 120 min and for the expected impact of the hydrocarbon fire regime, the coating consumption should be increased by 1.5–2 times compared to the coating consumption for the standard regime.

Keywords: oil and gas facility; steel structure; fire resistance limit; fire protection; hydrocarbon and standard fire regimes; intumescent coating; epoxy coating; cryogenic exposure

Citation: Gravit, M.; Shabunina, D.; Shcheglov, N. Thermal Characteristics of Epoxy Fire-Retardant Coatings under Different Fire Regimes. *Fire* **2023**, *6*, 420. https://doi.org/10.3390/fire6110420

Academic Editor: Pinghua Zhu

Received: 1 October 2023
Revised: 22 October 2023
Accepted: 30 October 2023
Published: 2 November 2023

1. Introduction

Safety problems in the industrial sphere are relevant all over the world. Oil and gas facilities characterized by the presence of large quantities of explosive substances and materials, process equipment and pipelines and significant horizontal and vertical distances are high-risk production facilities. Uncontrolled development of accident scenarios at oil and gas facilities involving explosions and fires may result in significant damage and loss of life. Risk assessment is one of the required components of safety assurance, which is conducted to identify individual hazards and assess their impact on the possible damage that may be caused to the population and the environment [1,2].

The development and improvement of fire risk assessment methodology for substances used at oil and gas facilities allow for predicting the consequences of fires and explosions and provide the necessary fire protection measures more accurately [3,4]. In [5], a refinery fire risk assessment using a multi-stage early warning and fire mitigation system was conducted; monitoring methods for the efficient and safe operation of the refinery such as control, forecasting and strategic planning with advance warning were proposed. In [6], an assessment of fire, explosion and the dispersion of toxic gas was conducted on the example of an onshore station to determine the effectiveness of the design protection systems. In [7], the fire safety of oil and gas pipelines and power lines was assessed, and the hazard level of each object was determined.

Steel, as a material for building structures at oil and gas facilities, is widely used in construction due to its ductility and high strength properties, as well as ease of installation and stability [8]. However, the high thermal conductivity and low specific heat capacity of steel combined with a low flexibility led to a rapid temperature increase in steel elements after fire exposure. Steel structures at oil and gas facilities during an accident are subjected to a high-temperature impact and overpressure according to the hydrocarbon regime, where the temperature reaches more than 1000 °C in the first minutes of the fire [9]. The strength of an unprotected steel structure decreases significantly in the 400–600 °C range, and the structure loses stability almost immediately when loaded. In this regard, oil and gas facilities should use structures capable of withstanding high-temperature effects, i.e., protected by fire protection means [10].

There are three main methods of fire protection of steel structures: intumescent coatings, plaster compositions or structural fire protection of structures [11–13]. Figure 1 presents a scheme of the means and methods of fire protection of steel structures [10].

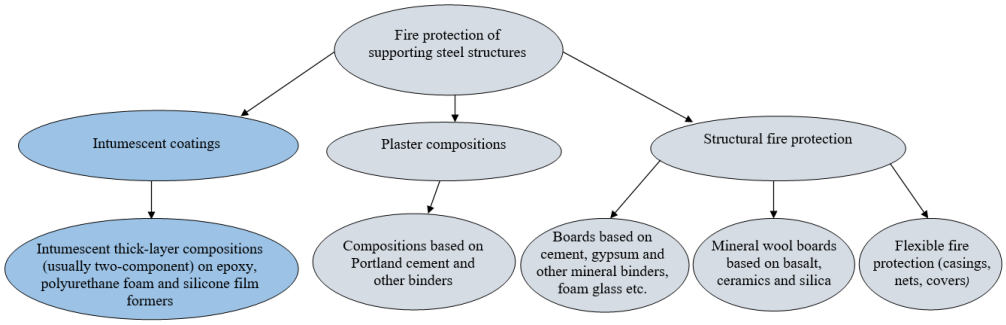

Figure 1. Main means and methods of fire protection of steel structures.

Structural fire protection is often applied in harsh climatic conditions. For example, in [10], experiments concerning steel structures with structural fire protection using basalt superfine fibers as an example in the Arctic region were demonstrated; an assessment of various fire protection means was conducted, the results of which showed that the most effective coatings for severe Arctic conditions are materials containing basalt superfine fibers based on basalt superfine fibers. In [14], research on structural curved fire protection to increase the fire resistance limit of building structures used at oil and gas facilities was presented.

The second method of fire protection of metal structures includes plaster compositions with a thickness of 10–60 mm, used in dry rooms (at a relative air humidity of less than 65%), applied on a steel grid and used to increase the fire resistance limit of metal structures up to 2 and more hours. In [15], experiments concerning clay and lime plaster compositions with a high density applied to wooden structures were demonstrated to determine their thermophysical properties under standard temperature conditions. Experimental studies are confirmed by numerical simulation, and the low fire protection efficiency of clay and lime plaster was shown. In [16], experimental studies of the properties of perlite plaster, gypsum fire-retardant boards and blowing coatings for steel elements in a real fire with heating and subsequent cooling rates of 10 K/min and 20 K/min were presented; the specific heat capacity and thermal conductivity of the selected fire-retardant materials were investigated. In [17], steel I-beam sections with a plaster fire-retardant coating were tested under hydrocarbon fire regime conditions with a fire protection efficiency of 120 min; temperature dependencies throughout the fire test were obtained.

The third method of fire protection includes intumescent coatings, which occupy a huge share as passive fire protection for structures worldwide [18]. Intumescent coating is a reactive chemical material that is used as the main fire protection material for steel structures. When the blowing coating is exposed to fire and heated above a critical temperature, the decomposition products of the main components of the blowing coating react with each other and release gases, which allows the coating to swell and form a lightweight

flame-retardant foam coke that protects the steel structure from the action of heat flux or flame [19,20].

Intumescent coatings are divided into solvent-free, solvent-based and water-based coatings [21]. Water-based coatings are mainly used for interior applications due to their vulnerability to moisture, while solvent-based coatings are less susceptible to water absorption and are used for exterior applications. Both types often use vinyl acetates or acrylics as binders. Solvent-free coatings with 100% dry residue are two- or three-component chemically cured coatings, which include intumescent coatings that are designed for high-risk applications such as petrochemical plants and offshore oil drilling platforms. Intumescent systems are usually two-component systems: the resin is mixed with a hardener and immediately applied to the steel structure. Due to the epoxy resin, the coatings dry quickly after application and are characterized by resistance to chemical and climatic influences, excellent adhesion, high repairability and have the highest possible fire resistance of structures among coatings [22]. For these reasons, intumescent coatings meet the high safety requirements for oil and gas construction (Figure 2).

Figure 2. Steel structures with intumescent fire-retardant coating on trestles of oil and gas terminal in Vysotsk, Russia. Photo by the authors.

Also, intumescent compositions have been confirming their durability and reliability under various fire regimes in marine conditions for many years [23]. In [24], a methodology for evaluating the fire protection effectiveness of intumescent coatings for steel structures exposed to high-temperature gas flows was developed and an experimental evaluation of the fire protection effectiveness of various intumescent coatings was conducted; a significant decrease in the fire protection effectiveness was shown when exposed to a high-temperature gas flow that promotes the development of a hydrocarbon fire regime. In [25], the compatibility of the intumescent coating and thermal properties of the coating using thermal insulation characteristics and thermogravimetric analysis was presented; the influence of the primer type and topcoat of the intumescent composition on the performance of the coating system was established. The study of [26] aimed to evaluate the durability of foam-coated intumescent coatings on steel panels during fire exposure under a hydrocarbon fire regime using the monitoring of the physical integrity, mechanical stability and thermal insulation capacity. In [27], two intumescent compositions were investigated to understand the potential failure mechanism of the primer. The analysis was conducted using a gas test furnace, a specially designed electrically heated furnace and thermogravimetric analysis. In [28], silicone-based intumescent coatings containing expandable graphite were developed and studied, and good physical fire-retardant properties were obtained under both standard and hydrocarbon fire regimes; a two-dimensional numerical model of intumescent coating behavior during fire was developed. In [29], it is

stated that blowing coatings are one of the effective means of the passive fire protection of steel structures in high-risk conditions at oil and gas facilities and offshore platforms.

In accidents at oil and gas facilities, intumescent fire protection shows its effectiveness. For example, the authors cite, in Figure 3, photos from a real fire at a large oil refinery in Russia, where steel structures were protected with intumescent coating. The foam core coating was preserved on the surface of the structure and the steel structure did not collapse and remained stable. It should be noted that the thickness of the charred blowing layer (foam coke) is small and is not more than 50 mm, which corresponds to the optimal thickness of foam coke for blowing compositions [18,30].

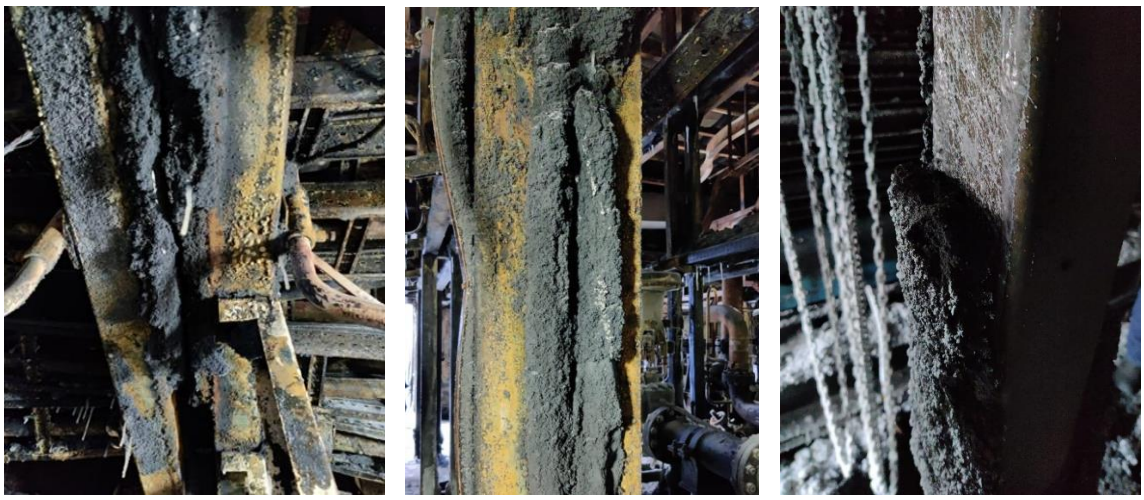

Figure 3. Steel structures with intumescent fire protection with foam coke formed after a fire in a production plant.

Fire-retardant intumescent coatings are two-component compositions of a polymer composition based on epoxy resin with mineral and target fillers and polyamide hardener, which is a homogeneous viscous liquid [19,31]. Functional fillers are a trade secret of manufacturers; however, as a rule, the flame-retardant composition includes epoxy resin (uncured dianic resin, for example, DER-331 or ED-20 grades), constituting 20.0–37.0% of the coating weight, then an exemplary composition of the following ingredients: ammonium polyphosphate, melamine, titanium whitewash, antimony oxides, aluminum hydroxide and graphite. Carbon nanotubes and glass spheres are also used as additives to reduce the fire hazard of coatings [18]. In standard tests, intumescent coatings emit quite caustic smoke, unlike acrylic soluble compositions, and transform into a dense and rigid foam coke, which allows them to provide high fire resistance in structures [27]. In the case of flame-retardant intumescent coatings, the components must be carefully selected. Then, it is necessary to ensure the processability of the material to make it finely dispersed and homogeneous by grinding in bead mills. The choice of components of the composition is important, for example, in the task of obtaining quality foam coke: rigid, with good adhesion, with closed cells and high-density foam coke, because even if all the tasks are met, the foam coke is formed, the coating has adhesion and in general, the required physical and mechanical characteristics are satisfactory, then, during testing, the foam coke may behave unpredictably and be formed in a chaotic order, in connection with which, the fire protection effectiveness will be low. Figure 4 shows photographs from an experimental study of an intumescent-coated steel column where the proportion of ammonium polyphosphate was greater than 25% and there was no reinforcing mesh used to contain and uniformly develop the foam coke.

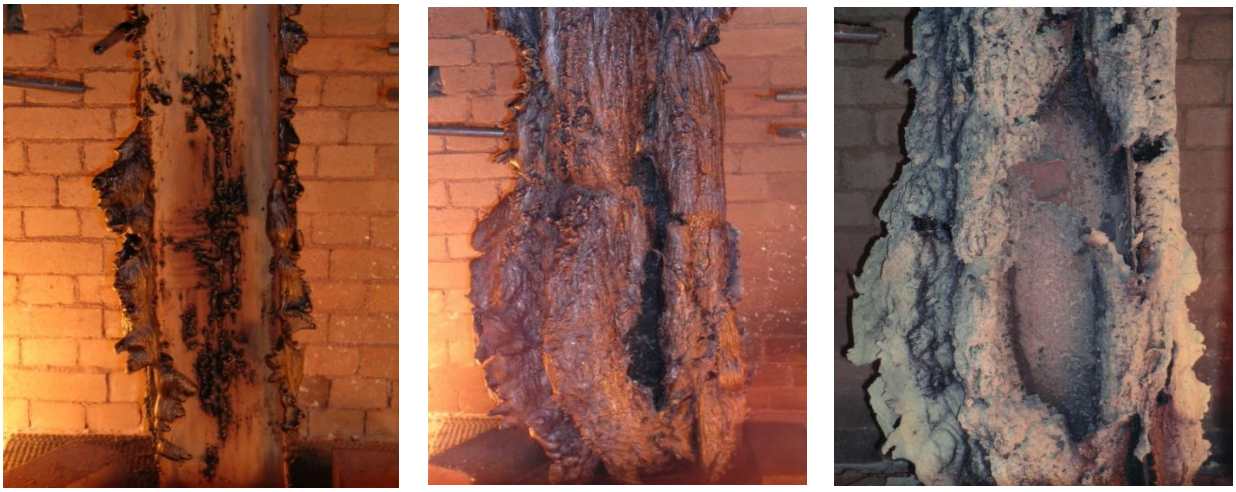

Figure 4. Fire-retardant intumescent coating without reinforcing mesh at 25 min of fire exposure.

The technology of applying a fire-retardant coating to the surface of metal structures also affects the fire protection efficiency of the coating and the fire resistance limits of the structure. In general, it is assumed that the fireproofing composition is applied layer by layer and evenly over the entire surface of the protected structure with an intermediate drying procedure (lasting at least 4 h at ambient temperature +20 °C), conducted before the application of each additional (starting from the second) layer; if the design thickness of the fireproofing coating is 6 mm or more, on the treated surface of all external corners (ribs) of the structure, a reinforcing glass mesh is laid over the uncured layer of the fireproofing composition (Figure 5) [32].

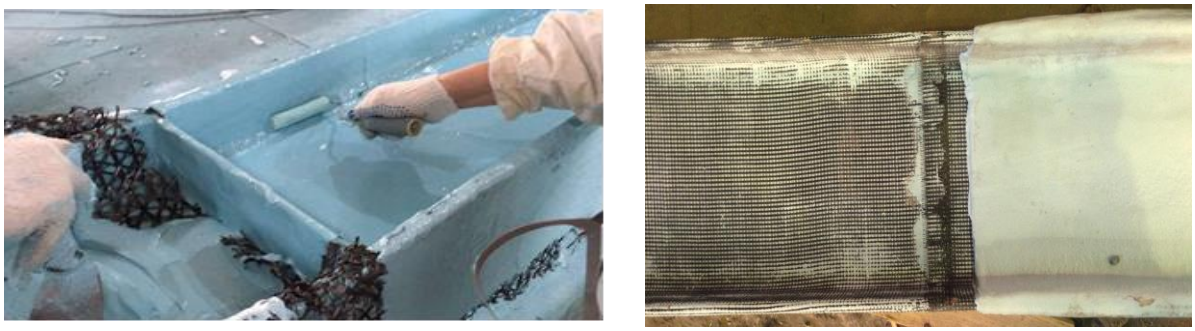

(**a**) (**b**)

Figure 5. The process of layer-by-layer application of intumescent fire-retardant coatings: (**a**) FireTex; (**b**) Chartek on the surface of metal structures using reinforcing mesh. Photo by the authors.

Numerical simulation is used to predict the fire behavior of building structures and to obtain temperature distributions [33–36]. For the simulation of the thermophysical processes of steel structures, the authors used the software package (SP) QuickField 6.6 [37]; the possibility of the numerical simulation of the fire resistance of building structures has been repeatedly confirmed by the authors of scientific papers. For example, in [34], temperature fields under the fire exposure of modern windows and elements of facade glazing were considered; it is shown that SP Elcut (QuickField 6.6) allows for predicting the behavior of building structures at an elevated temperature and displays the temperature distributions and stress fields. In [36], the simulation of the heating of structures of offshore stationary platforms was presented, which showed good correlation with the experimental results; the consumption of mineral boards for the bulkhead structure was predicted and the parameters of the thermal conductivity and heat capacity of the applied fire protection in the temperature range from 0 to 1000 °C were specified. In [35], the results of large-

scale fire tests of lightweight thin-walled steel structures for fire protection performance were presented. In [38], the simulation of the heating of steel structures with intumescent coating was presented to predict the behavior of the structure with applied fire-retardant composition and further experimental study.

The problem with the simulation of structural elements with blowing paint is the non-uniform transition during heating from intumescent coating to foam coke formation [38,39]. It is assumed that the foam coke is uniformly distributed over the column in time. This approach is not analogous to the behavior of plaster compositions when the simulation is divided into three parts: before, during and after the phase transition of water to vapor (evaporation), which takes place on the heating curve at about 100 °C, with the duration of this phase in time depending on the moisture content of the material [40]. Foam coke formation generally occurs from the 3rd minute of fire exposure and is completed in an average of 15–20 min. After the formation of stable carbon foam, the foam coke can be taken as a cellular structural element enveloping the building structure with a thickness of 30–40 mm (average thickness of foam coke for intumescent coatings) [18]. Figure 6 shows the increase in the foam coke during the experimental study in the muffle furnace.

Figure 6. Foam coke formation during the experiment in a muffle furnace [18].

Directly, the requirements of the fire protection efficiency of intumescent coatings and for ensuring the required fire resistance limits of structures at the facility (platforms, trestles) at the oil and gas complex are established in the design documentation for the facility. One of the important regulatory documents for this aspect of the reliability of structures is API 2218 [41], which establishes requirements not only for determining the fire protection effectiveness of fire protection products under a hydrocarbon fire regime, but also under cryogenic exposure, which simulates spills of liquefied hydrocarbons. As a rule, the limits of the fire resistance of structures are set by the load-bearing capacity for structures of 45, 60, 90 and 120 min. In Russia, SP 4.13130 [42] has been developed for these purposes, but there are no instructions for testing in a hydrocarbon regime, only in a standard regime, and there are no requirements for cryogenic effects. However, foreign designers of oil and gas chemical production facilities require fire protection products to confirm high parameters of fire protection effectiveness at 90 and 120 min in the hydrocarbon regime of fire, as well as the results of tests under cryogenic exposure. Thus, Russian manufacturers of fire protection materials test their materials haphazardly, voluntarily, according to their own methods and on different structures according to the requirements of the project at a particular facility at the oil and gas complex [10].

This paper presents studies of globally widely used intumescent coatings from six well-known manufacturers, which are on the supplier lists of major oil and gas companies. Several coatings were tested under standard fire regimes only, and some coatings were dipped in liquid nitrogen (cryogenic exposure) before exposure to a standard fire regime.

The purpose of this paper is to obtain averaged values of the thermophysical characteristics of intumescent compositions by solving the task of inverse thermal conductivity to predict their flame-retardant effectiveness under fire exposure under both hydrocarbon and standard regimes. To achieve this purpose, a comparative analysis of the experimental data of the most common intumescent compositions used on steel structures at oil and gas complex facilities as fire protection has been conducted; models of the heating of sections of structures with fire protection have been created and the thermophysical characteristics

in a wide temperature range have been obtained. In the simulation of the structures, the dry layer thickness was used as the thickness of the fire protection in the first stage, and the average thickness of the formed foam coke (40 mm) was used for the second stage, with no intermediate iterations. It is also shown that to ensure the fire resistance of the structure under the hydrocarbon regime, it is necessary to double, on average, the consumption of the coating that was tested under the standard regime.

2. Materials and Methods

Experimental studies of intumescent compositions, "Ograx-SCE" ("Unihimtek", Russia), "Inflex FA-21" ("Morneftegazstroy", Russia), "Plamkor-5" (Holding "VMP", Russia), FIRETEX M-90 (Great Britain), Chartek 1709 (International Protective Coatings, Great Britain) and "Pregrad-EP" (Russia), were conducted. The following samples were selected for experimental studies: Sample No. 1.0 ("Ograx-SCE"), Sample No. 2.1–No. 2.8 ("Inflex FA-21"), Sample No. 3.1–No. 3.3 ("Plamkor-5"), Sample No. 4.0 (FIRETEX M-90), Sample No. 5.0 (Chartek 1709), Sample No. 6.0 ("Pregrad-EP"). All fire protection systems consisted of different grades of epoxy compatible primers, fire-retardant paint and polyurethane-finished coats. A 20 × 20 mm carbon fiber mesh was used on all samples, except for Sample No. 3,3, where a 50 × 50 mm carbon fiber mesh was used.

The tests of Samples No. 2.1–No. 2.4, No. 2.7, No. 3.1–No. 3.3 and No. 4.0 were conducted until reaching the time of critical state in the process of fire exposure under the condition of creating a hydrocarbon temperature regime in the furnace fire chamber according to EN 1363-2:1999 [43], characterized by dependence (1):

$$T - T_0 = 1080 \times \left(1 - 0.325 \times e^{-0.167t} - 0.675 \times e^{-2.5t}\right). \quad (1)$$

where T means the temperature inside the furnace in °C, corresponding to the relevant time t; T_0 is the temperature in °C inside the furnace prior to the start of heat impact; t is the time in minutes from the start of the test.

Samples No. 2.5, No. 2.6 and No. 2.8 were tested according to the standard temperature regime according to EN 1363-2:1999 [43], characterized by relationship (2):

$$T - T_0 = 345 \times \lg(8t + 1), \quad (2)$$

During the fire test under hydrocarbon and standard temperature regimes, the metal of the test samples reached the critical temperature of 500 °C as the limit state [44]. Preparation of samples for testing, conditions of fire tests, determination of limit states of structures and evaluation of experimental results are regulated in [45].

Samples No. 1.0, No. 5.0 and No. 6.0 were first exposed to cryogenic exposure, then removed from the fire furnace and tested under the hydrocarbon fire regime characterized by Equation (1).

The SP QuickField was used for the simulation of thermophysical processes of the considered steel structures [37].

2.1. Experiments on Steel Structures

Experimental studies of steel structures with 6 coatings (test samples of 15, as some coatings were tested on several samples under different conditions) were conducted; the main parameters of the samples are summarized in Table 1. Samples No. 2.1 and No. 2.2 were identical structures with different thicknesses of applied intumescent coating tested under hydrocarbon fire regimes. Two identical experiments were conducted to confirm the obtained results under the condition of creating a hydrocarbon fire regime in the furnace fire chamber for Samples No. 3.1 and No. 3.2 (20 × 20 mm carbon fiber mesh was used). For Sample No. 3.3, a carbon fiber mesh with dimensions of 50 × 50 mm was used. Tests of Samples No. 2.3–No. 2.8 were conducted to determine the difference between standard and hydrocarbon exposure on steel structures.

Table 1. Main parameters of samples with intumescent coatings.

Sample	Profile	Height, mm	Section Ratio, mm^{-1} [46]	Average Thickness, mm	Regime
Sample No. 1.0	□ 100 × 8 mm [47]	2700	134	11.50	cryogenics + hydrocarbon regime
Sample No. 2.1	I 50B2 [48]	1700	172	9.20	hydrocarbon regime
Sample No. 2.2	I 50B2	1700	172	8.40	hydrocarbon regime
Sample No. 2.3	I 14B1	1700	172	10.30	hydrocarbon regime
Sample No. 2.4	I 14B1	1700	172	14.44	hydrocarbon regime
Sample No. 2.5	I 14B1	1700	172	6.30	standard regime
Sample No. 2.6	I 14B1	1700	172	8.75	standard regime
Sample No. 2.7	I 50B2	1700	172	4.13	hydrocarbon regime
Sample No. 2.8	I 50B2	1700	172	4.00	standard regime
Sample No. 3.1	I 50B2	1700	172	11.20	hydrocarbon regime
Sample No. 3.2	I 50B2	1700	172	11.20	hydrocarbon regime
Sample No. 3.3	I 50B2	1700	172	11.20	hydrocarbon regime
Sample No. 4.0	I 30K1	2700	159	13.70	hydrocarbon regime
Sample No. 5.0	I 30K1	2700	159	10.60	cryogenics + hydrocarbon regime
Sample No. 6.0	∅100 × 8	2700	136	20.00	cryogenics + hydrocarbon regime

Samples No. 1.0, No. 5.0 and No. 6.0 were tested under the hydrocarbon fire regime after a 10 min cryogenic exposure (immersion of the sample in liquid nitrogen at −196 °C). The level of liquid nitrogen was maintained at 800 mm from the bottom of the reservoir, with the samples immersed in the liquid nitrogen at 750 mm. The level of liquid nitrogen was monitored using a thermocouple installed at a height of 800 mm from the bottom of the reservoir with refrigerant (Figure 7). The limit state under cryogenic exposure was taken as reaching the temperature of −60 °C in the metal of the sample.

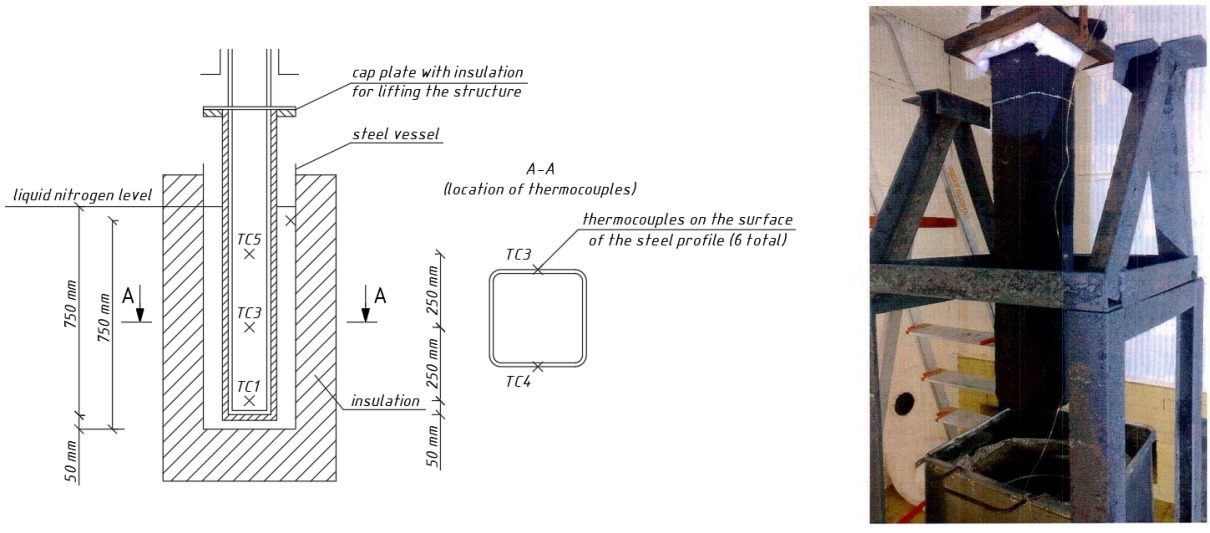

Figure 7. Installation of Samples No. 1.0, No. 5.0 and No. 6.0 for cryogenic experimentation.

After completion of cryogenic exposure, Samples No. 1.0, No. 5.0 and No. 6.0 were removed from the liquid nitrogen reservoir, inspected for coating defects and further subjected to fire exposure under hydrocarbon fire conditions.

2.2. Simulation in SP QuickField

All structural calculations in SP QuickField were performed using the finite element method.

To determine the characteristic of the fire protection ability of coatings of load-bearing steel structures, mathematical models of the heat conduction process were applied and the method of solving inverse tasks of heat conduction determined according to the system of Equations (3)–(6) was used [49,50].

- the equation of heat conduction:

$$c_\rho \rho_\rho \frac{\partial \theta_\rho}{\partial t} = \frac{\partial}{\partial x}\left(\lambda_\rho \frac{\partial \theta_\rho}{\partial x}\right), \tag{3}$$

$$0 < x < d_\rho; \theta_\rho = \theta_\rho(x,t); 0 < t < t_{max}$$

- initial condition:

$$\theta_\rho(x,0) = \theta_0, \tag{4}$$

- boundary condition on the outer surface of the inverse heat conduction task at $x = d_\rho$:

$$\lambda_\rho \frac{\partial \theta_\rho(d_\rho,t)}{\partial x} = \alpha^*\left[\theta_t - \theta_\rho(d_\rho,t)\right], \text{where} \tag{5}$$

$$\alpha^* = \alpha_c + \frac{C_0 \varepsilon}{\theta_t - \theta_\rho(d_\rho,t)}\left\{\left[\frac{\theta_t + 273.15}{100}\right]^4 - \left[\frac{\theta_\rho(d_\rho,t) + 273.15}{100}\right]^4\right\}$$

- boundary condition on the inner surface of the fireproof coating at $x = 0$:

$$\lambda_\rho \frac{\partial \theta_\rho(0,t)}{\partial x} = c_a \rho_a \times \frac{V}{A_p} \times \frac{\partial \theta_\rho(0,t)}{\partial t}, \text{ where} \tag{6}$$

x–coordinate in the fire protection coating ($x = 0$ corresponds to the point of contact between the coating and the metal where the sample is measured, temperature $\theta_a = \theta_\rho(0,t)$);

$c_\rho \rho_\rho$–specific heat capacity, J/(kg·K);

$\frac{V}{A_p}$–section ratio, mm^{-1};

λ_ρ–heat conductivity coefficient, W/(m·K);

t–time, s;

d_ρ–thickness of fireproof coating, mm;

t_{max}–the maximum heating time of the sample, s;

α_c–heat transfer coefficient on the outer surface of the fireproof coating, W/(m^2·K);

$$C_0 = 0.57;$$

$\varepsilon = 0.8$–the degree of blackness of the surface of the fire protection coating [51];

θ_0–initial temperature of the sample, °C;

θ_t–temperature in the firing furnace, °C.

Initial characteristics of steel: steel grade: C245 [52]; density 7800 kg/m^3; thermal conductivity and heat capacity are variable depending on temperature (values taken from the program reference book). The boundary conditions are presented in Table 2.

Table 2. Boundary conditions defined in SP QuickField.

Name of the Value	Value	Information Source
Convection heat transfer coefficient at hydrocarbon temperature regime, W/(m^2 · K)	50	[53]
Convection heat transfer coefficient at standard temperature regime, W/(m^2 · K)	25	[53]
Emissivity of steel	0.6	[54]
Initial ambient temperature, °C	20	-
Time step for calculating the temperature gradient of the structure, seconds	60	-

The simulation of the structure heating was performed in two phases:

(1) Analysis of the temperature increase on the steel sample under hydrocarbon and standard fire regimes after the start of fire exposure; during this time, the investigated intumescent coatings are still located on the samples;
(2) Analysis of temperature changes on the steel sample under hydrocarbon and standard fire regimes during the last minutes of fire exposure; during this time, a protective layer of 40 mm thick foam coke has already been formed around the samples (for simplicity, the thickness is averaged, and 40 mm is taken as optimal in terms of height and cell distribution).

Thermophysical properties of elements (thermal conductivity, heat capacity and density) at the first stage of the simulation are presented in Table 3. Geometric dimensions of the samples in the simulation are the same as the dimensions of the considered samples in the experimental study.

Table 3. Thermophysical properties of elements at the first stage of simulation.

Structural Elements	λ, W/(m·K)			C_p, J/(kg·K)			ρ, kg/m^3
	20 °C	100 °C	300 °C	20 °C	100 °C	300 °C	
Steel	49	25	25	469	670	670	7800
Air	0.0321	0.0915	0.0915	1009	1210	1210	1.275
Sample No. 1.0	0.08	0.07	0.07	1300	1300	1300	1200
Samples No. 2.1–2.8	0.07	0.08	0.08	600	850	900	700
Samples No. 3.1–3.3	0.20	0.17	0.15	1050	1050	1050	1220
Sample No. 4.0	0.15	0.10	0.09	800	800	800	1000
Sample No. 5.0	0.15	0.10	0.09	1000	1030	1080	1200
Sample No. 6.0	1.8	1.8	1.8	1100	1100	1100	700

The second stage of the simulation was based on the solution of the inverse task: the thermophysical properties of the formed foam coke at the last minutes of the tests were determined using the obtained experimental temperature–time dependences of the samples.

3. Results and Discussion

3.1. Experimental Results on Steel Structures

As a result of the cryogenic exposure of Sample No. 1.0, the average temperature of the sample did not drop more than 40 °C relative to its initial temperature. At the end of the cryogenic test, the average temperature of the sample was −18 °C. After the cryogenic test, the fireproofing coating had non-directional cracks with the width not more than 0.5 mm (Figure 8). In the process of the fire test, at the fourth minute, the formation of foam coke started, protecting the structure from heating. When the required time (120 min) was

reached, the test was terminated. The average temperature on the steel sample was 468 °C. The reaching of the critical temperature of 500 °C by Sample No. 1.0 was not recorded. It was found that Sample No. 1.0 provides fire-retardant effectiveness under the hydrocarbon regime of at least 120 min after 10 min of cryogenic exposure of the sample in the regime of full immersion in liquid nitrogen.

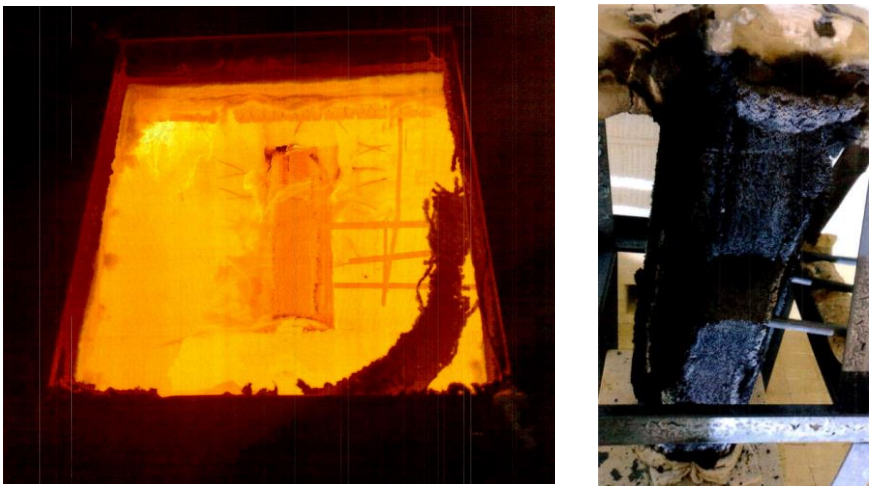

(**a**) (**b**)

Figure 8. Sample No. 1.0: (**a**) in the process of the experiment; (**b**) after the fire exposure.

The fire resistance limit of Sample No. 2.1 was reached at 124 min of fire exposure, due to reaching a critical temperature of 500 °C (Figure 9). The fire resistance limit of Sample No. 2.2 was reached at the 93rd minute of fire exposure, due to reaching a critical temperature of 500 °C. After completion of the thermal exposure, the formed foam coke on Samples No. 2.1 and No. 2.2 retained its structure and integrity (foam coke formation began at 10 min of fire exposure for Sample No. 2.1 and at the 8th minute for Sample No. 2.1). It was found that Samples No. 2.1 and No. 2.2 provide fire-retardant effectiveness under the hydrocarbon regime of at least 120 and 90 min, respectively.

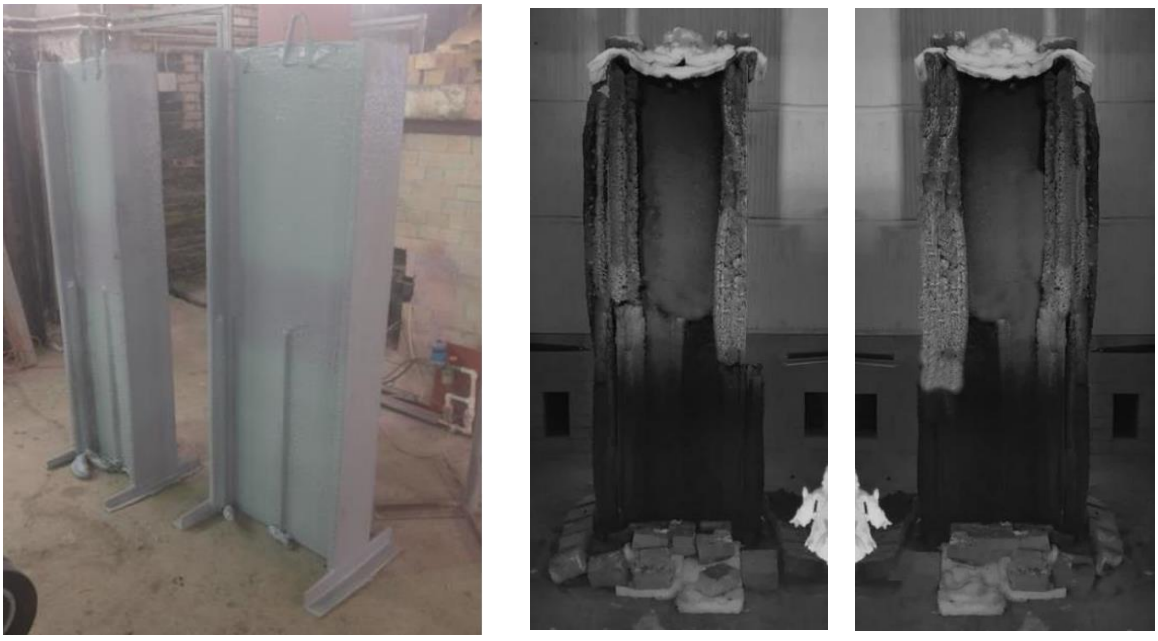

(**a**) (**b**)

Figure 9. Samples No. 2.1 and No. 2.2: (**a**) before the experiment; (**b**) after the fire exposure.

The fire resistance limit of Sample No. 2.3 was reached at 63 min of fire exposure, due to reaching a critical temperature of 500 °C. The fire resistance limit of Sample No. 2.4 was reached at the 124th minute of fire exposure, due to reaching a critical temperature of 500 °C. The fire resistance limit of Sample No. 2.7 was reached at the 94th minute of fire exposure, due to reaching a critical temperature of 500 °C. After completion of the thermal exposure, the formed foam coke on Samples No. 2.3, No. 2.4 and No. 2.7 retained its structure and integrity. It was found that Samples No. 2.3, No. 2.4 and No. 2.7 provide fire-retardant effectiveness under the hydrocarbon regime of at least 60, 120 and 90 min, respectively.

The fire resistance limit of Sample No. 2.5 was reached at 94 min of fire exposure, due to reaching a critical temperature of 500 °C. The fire resistance limit of Sample No. 2.6 was reached at the 123rd minute of fire exposure, due to reaching a critical temperature of 500 °C. The fire resistance limit of Sample No. 2.8 was reached at the 93rd minute of fire exposure, due to reaching a critical temperature of 500 °C. After completion of the thermal exposure, the formed foam coke on Samples No. 2.5, No. 2.6 and No. 2.8 retained its structure and integrity. It was found that Samples No. 2.5, No. 2.6 and No. 2.8 provide fire-retardant effectiveness under the standard regime of at least 90, 120 and 90 min, respectively.

The fire resistance limit of Sample No. 3.1 was reached at the 94th minute of fire exposure, due to reaching the critical temperature of 500 °C. At the 3rd minute of the test, the coating began to swell; at the 7th minute, the sample burned independently. The fire resistance limit of Sample No. 3.2 was reached in the 92nd minute of fire exposure, due to reaching a critical temperature of 500 °C. At the 3rd minute of the test, the coating began to swell; at the 10th minute, the sample burned independently. After completion of the thermal exposure, the formed foam coke on Samples No. 3.1 and No. 3.2 retained its structure and integrity. It was found that Samples No. 3.1 and No. 3.2 provide fire-retardant effectiveness under the hydrocarbon regime of at least 90 min.

As a result of the tests for Sample No. 3.3 with a 50 × 50 mm glass fiber mesh, coating bloating and independent combustion started in the 4th minute of the test (same as for Samples No. 3.1 and No. 3.2), but coating fragments started to fall at the 21st minute and the temperature reached the critical temperature of 500 °C at the 73rd minute (instead of the expected 90 min). Uneven mixing of the paint was assumed to be the cause (Figure 10). It was found that Sample No. 3.3 provides fire-retardant effectiveness under the hydrocarbon regime of at least 60 min.

Figure 10. Sample No. 3.3 at the end of the test.

The fire resistance limit of Sample No. 4.0 was reached at the 125th minute of fire exposure, due to reaching a critical temperature of 500 °C. After completion of the thermal exposure, the formed foam coke on Sample No. 4.0 retained its structure and integrity. It was found that Sample No. 4.0 provides fire-retardant effectiveness under the hydrocarbon regime of at least 120 min.

As a result of the cryogenic exposure of Sample No. 5.0, the average temperature of the sample did not drop more than 50 °C relative to its initial temperature. At the end of

the cryogenic test, the average temperature of the sample was −26 °C. After the cryogenic test, the fireproofing coating had non-directional cracks with the width not more than 0.5 mm. In the process of the fire test, at the 5th minute, the formation of foam coke started, protecting the structure from heating. The fire resistance limit of Sample No. 5.0 was reached at the 105th minute of fire exposure, due to reaching the critical temperature of 500 °C. It was found that Sample No. 5.0 provides fire-retardant effectiveness under the hydrocarbon regime of at least 90 min after 10 min of the cryogenic exposure of the sample in the regime of full immersion in liquid nitrogen.

As a result of the cryogenic exposure of Sample No. 6.0, the average temperature of the sample did not drop more than 40 °C relative to its initial temperature. At the end of the cryogenic test, the average temperature of the sample was −17 °C. After the cryogenic test, the fireproofing coating had non-directional cracks with the width not more than 0.5 mm. In the process of the fire test, at the 15th minute, the formation of foam coke started, protecting the structure from heating. When the required time (90 min) was reached, the test was terminated. The average temperature on the steel sample was 450 °C (Figure 11). The reaching of the critical temperature of 500 °C by Sample No. 6.0 was not recorded. It was found that Sample No. 6.0 provides fire-retardant effectiveness under the hydrocarbon regime of at least 90 min after 10 min of the cryogenic exposure of the sample in the regime of full immersion in liquid nitrogen.

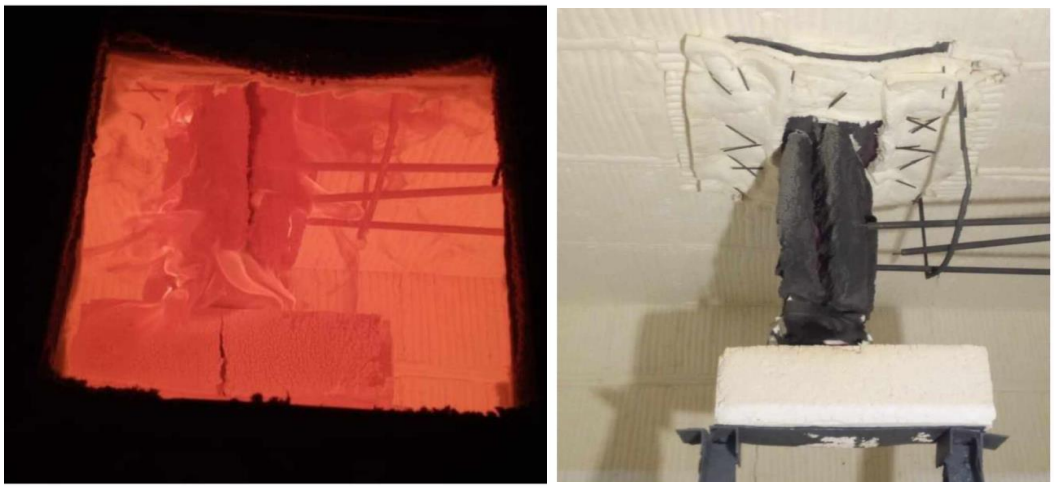

(**a**) (**b**)

Figure 11. Sample No. 6.0: (**a**) in the process of the experiment; (**b**) after the fire exposure.

Figure 12 shows the time–temperature curves of the intumescent-coated steel columns during the fire tests (for Samples No. 1.0, No. 5.0 and No. 6.0 initially exposed to cryogenic exposure, the start and end times of cryogenic exposure and the start of fire exposure are shown). Figure 12 shows the averaged readings of the thermocouples located at the mid-height of the samples.

As can be seen in Figure 12, the graphs are divided into two groups: coatings that were initially cryogenically exposed and then subjected to the hydrocarbon fire regime (Samples No. 1.0, No. 5.0 and No. 6.0), and coatings that were not cryogenically exposed (Samples No. 2.1–No. 2.8, No. 3.1–No. 3.3 and No. 4.0). In the first case, the average dry layer thickness of the coatings on the samples (14 mm) exceeded the average dry layer thickness of the coatings in the second case (10 mm) (Table 4). Sample No. 4.0, which had the maximum coating thickness of the samples exposed only to fire, shows the smoothest temperature increase throughout the experimental study and demonstrates fire-retardant effectiveness for 120 min. Sample No. 1.0, exposed to cryogenic exposure before the fire test, shows the smoothest increase in temperature after cryogenic exposure of the sample and demonstrates fire-retardant effectiveness for 120 min. Samples No. 2.1 and No. 2.2,

which have the smallest coating thicknesses under the hydrocarbon regime of fire, show a rapid temperature increase from the first minutes of the test, slowing down after the formation of the protective foam coke layer.

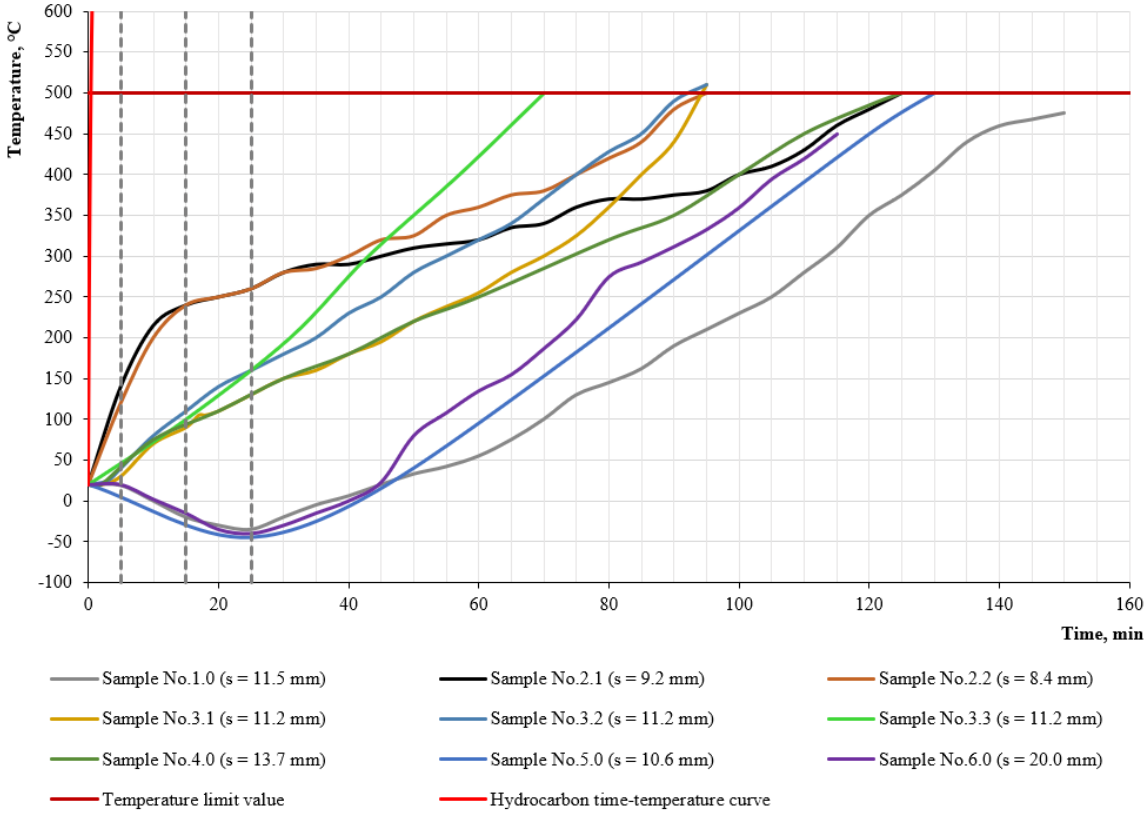

Figure 12. Temperature curves of samples during fire tests and cryogenic exposure (for Samples No. 1.0, No. 5.0 and No. 6.0).

Table 4. Results of tests of intumescent fire-retardant coatings.

Sample	Profile	Section Ratio, mm^{-1} [46]	Average Thickness, mm	Cryogenic Exposure	Fire Protection Effectiveness, min
Sample No. 1.0	□ 100 × 8 mm [47]	134	11.50	+	120
Sample No. 2.1	I 50B2 [48]	172	9.20	–	120
Sample No. 2.2	I 50B2	172	8.40	–	90
Sample No. 2.3	I 14B1	172	10.30	–	60
Sample No. 2.4	I 14B1	172	14.44	–	120
Sample No. 2.5	I 14B1	172	6.30	–	90
Sample No. 2.6	I 14B1	172	8.75	–	12-
Sample No. 2.7	I 50B2	172	4.13	–	90
Sample No. 2.8	I 50B2	172	4.00	–	90
Sample No. 3.1	I 50B2	172	11.20	–	90
Sample No. 3.2	I 50B2	172	11.20	–	90
Sample No. 3.3	I 50B2	172	11.20	–	60
Sample No. 4.0	I 30K1	159	13.70	–	120
Sample No. 5.0	I 30K1	159	10.60	+	90
Sample No. 6.0	∅100 × 8	136	20.00	+	90

As can be seen from Figure 12 and Table 4, the average value of thickness for intumescent coatings to ensure a fire protection effectiveness of 120 min is about 12 mm. The variation in the obtained results does not exceed 20%, which, of course, can be explained by the similarity of the formulations. The difference consists in the quality of meshes, production technology and the quality of paint layer application.

The thickness of the foam coke in relation to the average thickness of the initial coating was not recorded in any of the test reports. Apparently, this is caused by the fact that the structure is left to cool in the furnace and disassembled the next day and then simply disposed of. However, the photographs show that in the final minutes of the tests, the value of the foam coke as a thermal insulating layer relative to the geometric characteristics of the structures can be taken as 40 mm on average.

Figure 13 shows the time–temperature curves of steel Samples No. 2.3–No. 2.8 under standard and hydrocarbon fire regimes.

According to the observations of the experimental studies of Samples No. 2.3, No. 2.4 and No. 2.7, the foam coke formation was completed in the interval of 6–10 min. For Sample No. 2.5, the time of foam coke formation under the standard fire regime is in the range of 36–42 min, for Sample No. 2.6, in the range of 55–60 min and for Sample No. 2.8, in the range of 37–45 min. As can be seen from Figure 13, an optimal coating thickness of about 8–9 mm is required to provide a fire protection effectiveness of at least 120 min under the standard regime, while an optimum coating thickness of about 14–15 mm is required when exposed to the hydrocarbon regime of fire. Also, fire-retardant coatings on samples tested under the hydrocarbon regime (Samples No. 2.3, No. 2.4 and No. 2.7) were applied in two layers with the use of reinforcing carbon fiber mesh with a mesh size of 20 × 20 mm. Fire-retardant coatings on the samples tested under the standard fire regime (No. 2.5, No. 2.6 and No. 2.8) were applied in one layer without reinforcing mesh.

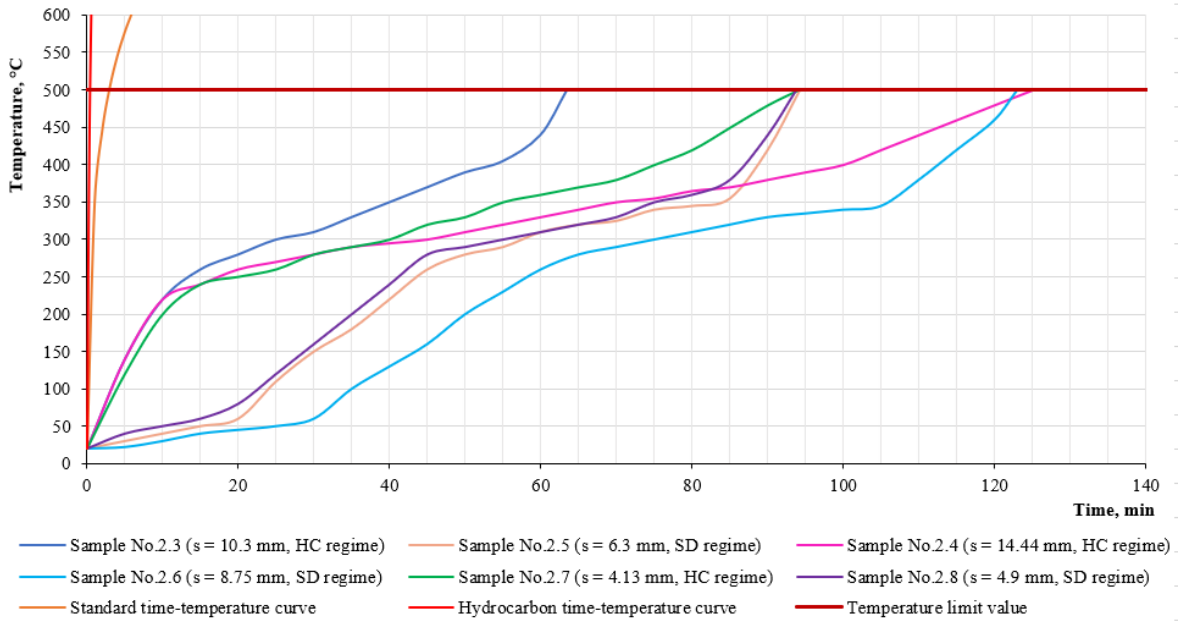

Figure 13. Temperature curves of Samples No. 2.3–No. 2.8 during fire tests under standard and hydrocarbon regimes.

3.2. Results of Simulation in SP QuickField

As a result of the simulation, visualizations of the heating of the samples of steel columns with intumescent coatings and a temperature dependence on time at the points of thermocouple location on the surface of the experimental samples under the hydrocarbon regime of fire were obtained (Figures 14 and 15). The graph shows the averaged readings

of thermocouples located in the middle of the height of the samples (25 min is the start of the fire testing for samples initially exposed to cryogenic exposure).

As can be seen in Figure 15, the graph for Sample No. 2.2, which has a coating thickness of 8.4 mm, grows at a higher rate until the temperature reaches 220 °C during the first 10 min of the experiment, characterized by the end of the formation of the foam coke layer. Furthermore, the heating of Sample No. 2.2 is characterized by uniform growth up to the critical temperature of 500 °C. Compared to the graphs for Samples No. 1.0 and No. 3.1, which have comparable coating thicknesses (11.5 mm and 11.2 mm, respectively) but a higher density (300 kg/m^3 and 310 kg/m^3 compared to 220 kg/m^3) and thermal conductivity of the formed foam coke (Tables 4–6), the graph for Sample No. 2.2 grows at a slower rate. The graph for Sample No. 1.0 shows a smoother temperature change over time from the cryogenic and fire effects until the end of the test at the 150th minute.

Table 5. Thermal properties of foam coke on Sample No. 1.0.

T, °C	**100**	**200**	**300**	**400**	**500**	**600**	**700**	**800**	**900**	**1000**	**1100**
λ, W/K·m	0.07	0.071	0.072	0.073	0.074	0.08	0.09	0.10	0.11	0.13	0.15
C, J/kg·m	800	825	850	880	900	925	955	980	990	1000	1010

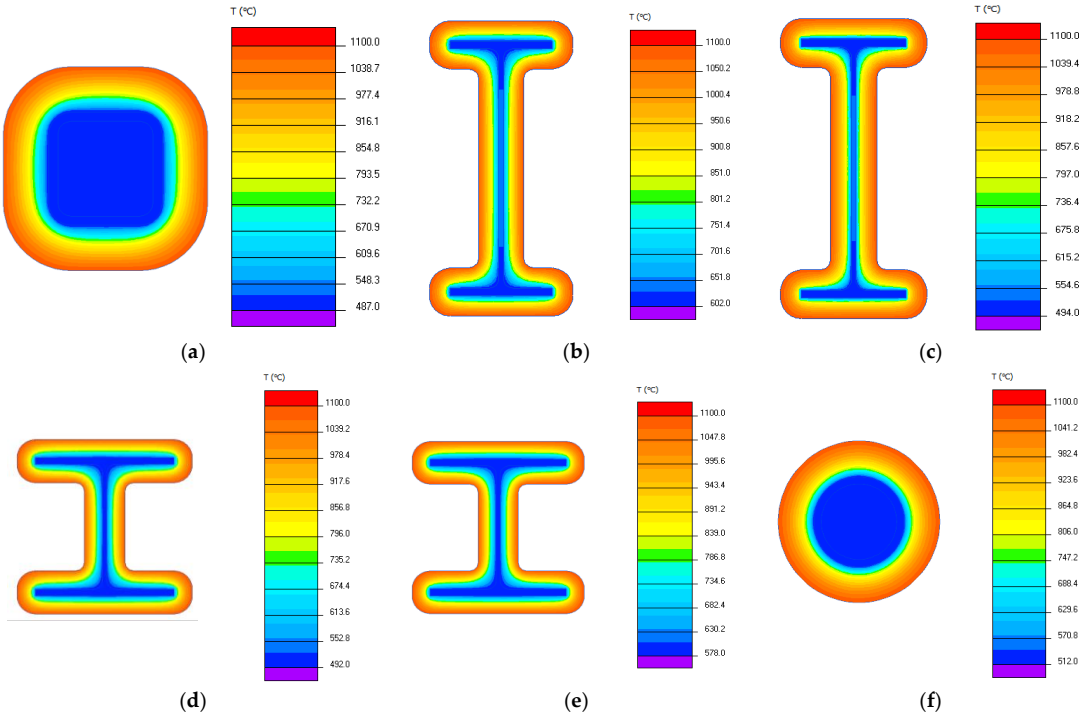

Figure 14. Visualizations of sample heating: (**a**) Sample No. 1.0; (**b**) Sample No. 2.1; (**c**) Samples No. 3.1 and No. 3.2; (**d**) Sample No. 4.0; (**e**) Sample No. 5.0; (**f**) Sample No. 6.0.

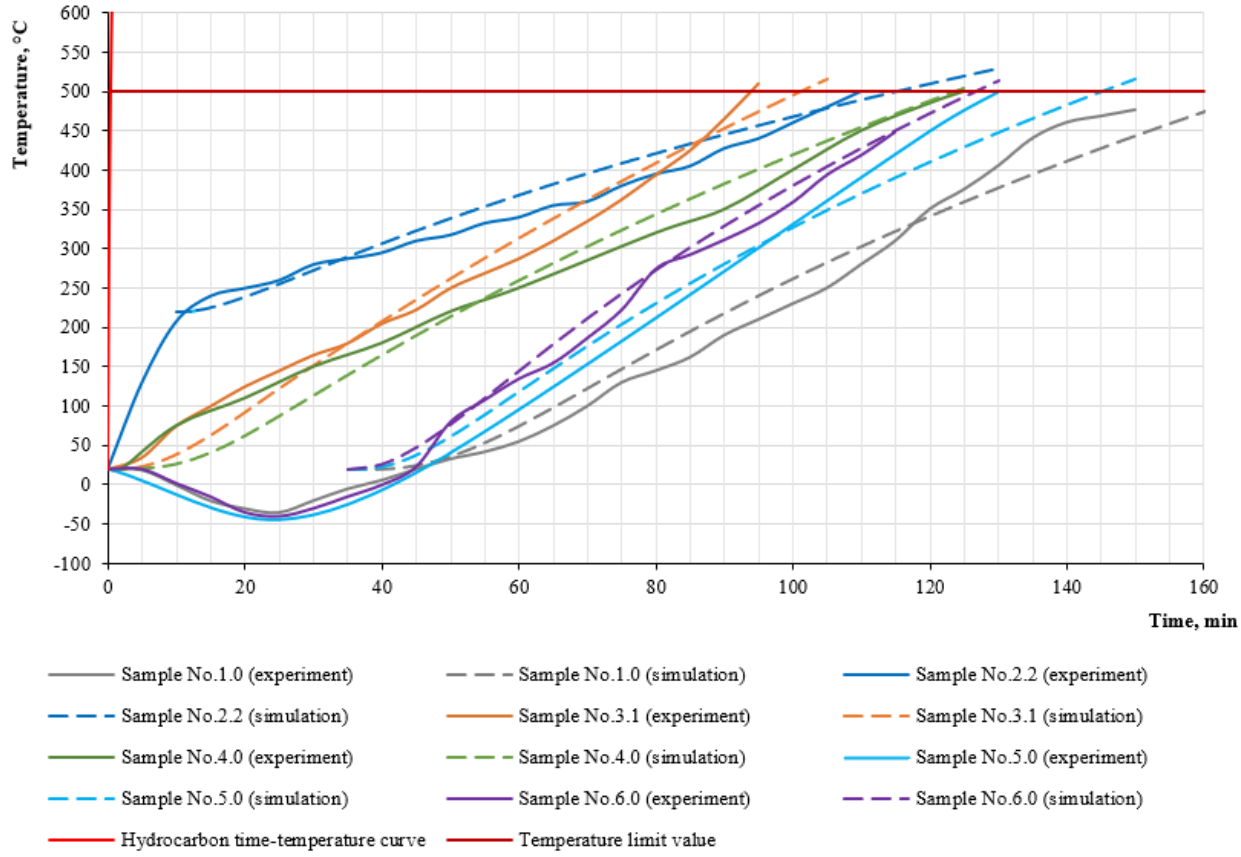

Figure 15. Experimental and calculated temperature curves of samples during fire exposure under hydrocarbon fire regime.

Table 6. Thermal properties of foam coke on Sample No. 2.2.

T, °C	100	200	300	400	500	600	700	800	900	1000	1100
λ, W/K·m	0.12	0.09	0.07	0.055	0.05	0.048	0.046	0.046	0.048	0.05	0.055
C, J/kg·m	700	745	780	830	850	875	915	950	990	1000	1020

According to the results of solving the inverse task in SP QuickField 6.6, the thermophysical properties of the formed foam coke were determined (Tables 5–10). Figures 8–11 show visualizations of the samples heating up at the end of the fire tests, from which a graph of the temperature–time dependence for the sample coatings on the experimental and calculated values is plotted (Figures 12–15), from which it is possible to make a direct comparison of Samples No. 1.0, No. 2.2 and No. 3.1, which have approximately the same thicknesses (11.5/8.4/11.2 mm) and section ratios (134/172/172 mm^{-1}).

Table 7. Thermal properties of foam coke on Sample No. 3.1.

T, °C	100	200	300	400	500	600	700	800	900	1000	1100
λ, W/K·m	0.15	0.15	0.1	0.05	0.05	0.05	0.08	0.14	0.2	0.25	0.3
C, J/kg·m	600	600	600	400	200	200	200	200	300	600	900

Table 8. Thermal properties of foam coke on Sample No. 4.0.

T, °C	**100**	**200**	**300**	**400**	**500**	**600**	**700**	**800**	**900**	**1000**	**1100**
λ, W/K·m	0.04	0.05	0.05	0.05	0.06	0.08	0.11	0.14	0.16	0.17	0.19
C, J/kg·m	820	840	860	890	900	930	980	1040	1120	1200	1300

Table 9. Thermal properties of foam coke on Sample No. 5.0.

T, °C	**100**	**200**	**300**	**400**	**500**	**600**	**700**	**800**	**900**	**1000**	**1100**
λ, W/K·m	0.1	0.09	0.089	0.09	0.1	0.11	0.12	0.13	0.15	0.17	0.2
C, J/kg·m	1030	1050	1080	1090	1100	1120	1140	1150	1170	1180	1200

Table 10. Thermal properties of foam coke on Sample No. 6.0.

T, °C	**100**	**200**	**300**	**400**	**500**	**600**	**700**	**800**	**900**	**1000**	**1100**
λ, W/K·m	0.14	0.12	0.11	0.09	0.08	0.08	0.09	0.12	0.16	0.20	0.25
C, J/kg·m	800	815	830	840	850	860	870	880	890	900	910

3.3. Discussion

Based on the thermophysical properties of the samples in the first simulation phase (at the beginning of the test), it can be noted that Sample No. 1.0, which initially has a higher heat capacity and lower thermal conductivity compared to Sample No. 2.2 and to Samples No. 3.1 and No. 3.2, beginning at the 15th minute, forms a foam coke layer protecting the structure with higher values of density and heat capacity and with a lower value of thermal conductivity relative to the sample of Samples No. 2.2, No. 3.1 and No. 3.2, indicating the better fire protection effectiveness of Sample No. 1.0 (120 min) compared to the fire resistance of Sample No. 2.2 and Samples No. 3.1 and No. 3.2 (90 min) under the hydrocarbon regime of fire. In turn, Sample No. 3, which has a similar section ratio (172 mm^{-1}) with Sample No. 2, is characterized by a smooth and uniform temperature increase throughout the fire exposure, while Sample No. 2 has a rapid temperature increase at the initial time point, highlighting the fire protection effectiveness of Sample No. 3. All curves obtained from the experimental study and shown in Figure 13 have a similar character, which indicates the uniformity of the coatings in terms of the formulations, clearly separated areas of curves when exposed to the hydrocarbon regime (rapid temperature increase) and standard regime.

By interpolating and extrapolating the results of the experimental data of Samples No. 2.3–No. 2.8 (Figure 15), nomograms of the dependence of time to reach the critical temperature of the steel samples on the section ratio at different thicknesses of the dry layer were obtained. Nomograms are given for the samples tested under two fire regimes: hydrocarbon and standard (Figures 16 and 17).

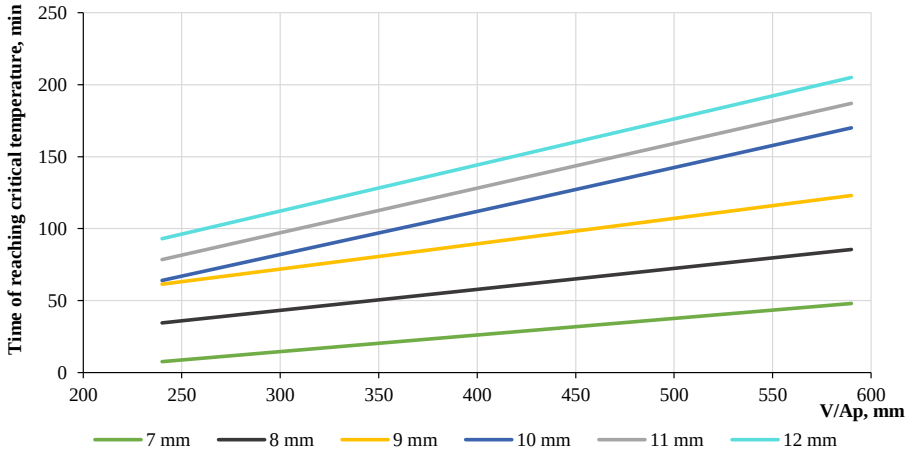

Figure 16. Dependence of time to reach critical temperature on section ratio in hydrocarbon fire regime of fire at different dry layer thicknesses.

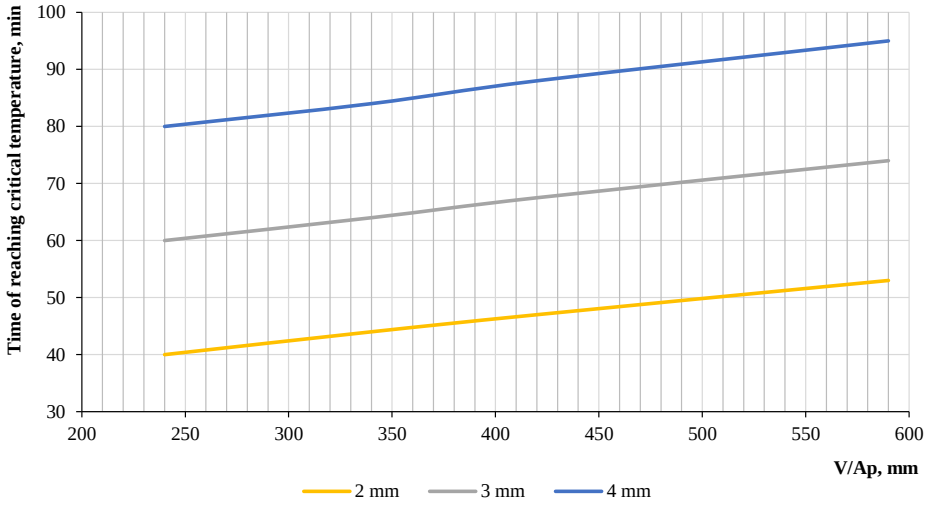

Figure 17. Dependence of time to reach critical temperature on section ratio in standard fire regime of fire at different dry layer thicknesses.

4. Conclusions

Intumescent flame-retardant coatings have a rather low reproducibility in experiments than structural fire protection, but their application on objects of industrial importance will increase, primarily because of the high technological efficiency of the application.

As this study showed, it is necessary to have data on the flame-retardant effectiveness of coatings both with and without cryogenic exposure, since the values are obviously lower with cryogenic exposure, the behavior of the intumescent coating is different and the choice of the flame retardant will not be fully comparable with coatings from different manufacturers. Nomograms for fire-retardant coatings (graphs of «temperature–time» dependence for each given thickness of the structure) should also be developed both taking into account cryogenic spillage and the hydrocarbon fire regime and taking into account no spillage and only fire exposure to coatings with similar properties declared by manufacturers.

While the initial components of intumescent materials are quite the same, epoxy resin and polyamide hardener, it is the functional additives—flame retardants and combustion retardants—that give the compositions important and distinctive properties. If the formulation of the composition is sufficiently calibrated, it can be seen via experimentation that there are formulations that do have a serious fire-retardant effectiveness, achieving 120 min

with sufficiently long and smooth heating times. The average coating thickness should be 12 mm on average.

Simulation of blowing compositions is a certain difficulty (unlike structural boards and even plaster compositions), due to the inhomogeneity of the process of foam coke formation on a steel structure. Averaged values of the thermophysical characteristics of intumescent coating foams when their stabilization is complete have been obtained. The adopted assumptions of foam coke formation after release and stabilization as a cellular structure with low thermal conductivity and low density correlate well enough with the experimental data, which can be averaged for engineering calculations on the fire protection of structures.

Author Contributions: Conceptualization, M.G.; methodology, M.G.; software, N.S.; formal analysis, N.S.; data curation, D.S.; writing—original draft preparation, D.S. All authors have read and agreed to the published version of the manuscript.

Funding: This research was funded by the Ministry of Science and Higher Education of the Russian Federation within the framework of the state assignment No. 075-03-2022-010 dated 14 January 2022 (Additional agreement 075-03-2022-010/10 dated 09 November 2022, Additional agreement 075-03-2023-004/4 dated 22 May 2023), FSEG-2022-0010.

Institutional Review Board Statement: Not applicable.

Informed Consent Statement: Not applicable.

Data Availability Statement: Not applicable.

Conflicts of Interest: The authors declare no conflict of interest.

References

1. Gorlenko, N.V.; Murzin, M.A. Comparative Analysis of Fire Risks in Coal and Oil and Gas Industries. *IOP Conf. Ser. Mater. Sci. Eng.* **2019**, *687*, 066009. [CrossRef]
2. Makhutov, N.A.; Bolshakov, A.M.; Zakharova, M.I. Possible Scenarios of Accidents in Reservoirs and Pipelines at Low Operating Temperature. *Inorg. Mater.* **2016**, *52*, 1498–1502. [CrossRef]
3. Tong, S.J.; Wu, Z.Z.; Wang, R.J.; Wu, H. Fire Risk Study of Long-Distance Oil and Gas Pipeline Based on QRA. *Procedia Eng.* **2016**, *135*, 369–375. [CrossRef]
4. Ivanov, A.V.; Dali, F.A.; Ivakhnyuk, G.K.; Skripnick, I.L.; Simonova, M.A.; Shikhalev, D.V. Nanostructures Management Technology to Reduce the Fire Risk in the Oil and Gas Industry: Performance, Features and Implementation. *J. Appl. Eng. Sci.* **2021**, *19*, 84–91. [CrossRef]
5. Alam, M.Z.; Sakib, M.N.; Islam, M.; Jalal Uddin, M. Various Risks and Safety Analysis to Reduce Fire in Oil Refinery Plant. *IOP Conf. Ser. Mater. Sci. Eng.* **2021**, *1078*, 012028. [CrossRef]
6. Abdoul Nasser, A.H.; Ndalila, P.D.; Mawugbe, E.A.; Emmanuel Kouame, M.; Paterne, M.A.; Li, Y. Mitigation of Risks Associated with Gas Pipeline Failure by Using Quantitative Risk Management Approach; a Descriptive Study on Gas Industry. *J. Mar. Sci. Eng.* **2021**, *9*, 1098. [CrossRef]
7. Masoumi, Z.; van L. Genderen, J.; Maleki, J. Fire Risk Assessment in Dense Urban Areas Using Information Fusion Techniques. *ISPRS Int. J. Geo-Inf.* **2019**, *8*, 579. [CrossRef]
8. Kodur, V.K.R.; Naser, M.Z. Approach for Shear Capacity Evaluation of Fire Exposed Steel and Composite Beams. *J. Constr. Steel Res.* **2018**, *141*, 91–103. [CrossRef]
9. Gravit, M.; Gumerova, E.; Bardin, A.; Lukinov, V. Increase of Fire Resistance Limits of Building Structures of Oil-and-Gas Complex Under Hydrocarbon Fire. *Adv. Intell. Syst. Comput.* **2018**, *692*, 818–829. [CrossRef]
10. Gravit, M.; Shabunina, D. Structural Fire Protection of Steel Structures in Arctic Conditions. *Buildings* **2021**, *11*, 499. [CrossRef]
11. Elbasuney, S.; Maraden, A. Novel Thermoset Nanocomposite Intumescent Coating Based on Hydroxyapatite Nanoplates for Fireproofing of Steel Structures. *J. Inorg. Organomet. Polym. Mater.* **2020**, *30*, 820–830. [CrossRef]
12. Mahmud, H.M.I.; Mandal, A.; Nag, S.; Moinuddin, K.A.M. Performance of Fire Protective Coatings on Structural Steel Member Exposed to High Temperature. *J. Struct. Fire Eng.* **2021**, *12*, 193–211. [CrossRef]
13. Jiang, S.; Wu, H. An Experimental Investigation on the Fire Resistance of the Integrated Envelope-Fire Protection Material for Steel Buildings. *Prog. Steel Build. Struct.* **2021**, *23*, 77–84. [CrossRef]
14. Gravit, M.; Simonenko, Y.; Yablonskii, L. 3D-Flexible Intumescent Fire Protection Mesh for Building Structures. *E3S Web Conf.* **2019**, *91*, 02004. [CrossRef]
15. Johanna, L.; Judith, K.; Alar, J.; Birgit, M.; Siim, P. Material Properties of Clay and Lime Plaster for Structural Fire Design. *Fire Mater.* **2021**, *45*, 355–365. [CrossRef]

16. Zehfuß, J.; Sander, L.; Schaumann, P.; Weisheim, W. Thermal Material Properties of Fire Protection Materials for Natural Fire Scenarios. *Bautechnik* **2018**, *95*, 535–546. [CrossRef]
17. Gravit, M.V.; Golub, E.V.; Antonov, S.P. Fire Protective Dry Plaster Composition for Structures in Hydrocarbon Fire. *Mag. Civ. Eng.* **2018**, *79*, 86–94. [CrossRef]
18. Zybina, O.; Gravit, M. *Intumescent Coatings for Fire Protection of Building Structures and Materials*; Springer Series on Polymer and Composite Materials; Springer International Publishing: Cham, Switzerland, 2020.
19. Kandola, B.K.; Luangtriratana, P.; Duquesne, S.; Bourbigot, S. The Effects of Thermophysical Properties and Environmental Conditions on Fire Performance of Intumescent Coatings on Glass Fibre-Reinforced Epoxy Composites. *Materials* **2015**, *8*, 5216–5237. [CrossRef]
20. Jimenez, M.; Bellayer, S.; Revel, B.; Duquesne, S.; Bourbigot, S. Comprehensive Study of the Influence of Different Aging Scenarios on the Fire Protective Behavior of an Epoxy Based Intumescent Coating. *Ind. Eng. Chem. Res.* **2013**, *52*, 729–743. [CrossRef]
21. Morys, M.; Häßler, D.; Krüger, S.; Schartel, B.; Hothan, S. Beyond the Standard Time-Temperature Curve: Assessment of Intumescent Coatings under Standard and Deviant Temperature Curves. *Fire Saf. J.* **2020**, *112*, 102951. [CrossRef]
22. Yasir, M.; Amir, N.; Ahmad, F.; Ullah, S.; Jimenez, M. Effect of Basalt Fibers Dispersion on Steel Fire Protection Performance of Epoxy-Based Intumescent Coatings. *Prog. Org. Coat.* **2018**, *122*, 229–238. [CrossRef]
23. Gravit, M.; Klementev, B.; Shabunina, D. Fire Resistance of Steel Structures with Epoxy Fire Protection under Cryogenic Exposure. *Buildings* **2021**, *11*, 537. [CrossRef]
24. Andryushkin, A.Y.; Kirshina, A.A.; Kadochnikova, E.N. The Evaluation of the Fire-Retardant Efficiency of Intumescent Coatings of Steel Structures Exposed to High-Temperature Gas Flows. *Pozharovzryvobezopasnost/Fire Explos. Saf.* **2021**, *30*, 14–26. [CrossRef]
25. Mariappan, T.; Kamble, A.; Naik, S.M. An Investigation of Primer Adhesion and Topcoat Compatibility on the Waterborne Intumescent Coating to Structural Steel. *Prog. Org. Coat.* **2019**, *131*, 371–377. [CrossRef]
26. Naik, A.D.; Duquesne, S.; Bourbigot, S. Hydrocarbon Time-Temperature Curve under Airjet Perturbation: An in Situ Method to Probe Char Stability and Integrity in Reactive Fire Protection Coatings. *J. Fire Sci.* **2016**, *34*, 385–397. [CrossRef]
27. Nørgaard, K.P.; Dam-Johansen, K.; Català, P.; Kiil, S. Laboratory and Gas-Fired Furnace Performance Tests of Epoxy Primers for Intumescent Coatings. *Prog. Org. Coat.* **2014**, *77*, 1577–1584. [CrossRef]
28. Nyazika, T.; Jimenez, M.; Samyn, F.; Bourbigot, S. Modeling Heat Transfers across a Silicone-Based Intumescent Coating. *J. Phys. Conf. Ser.* **2018**, *1107*, 032012. [CrossRef]
29. Zeng, Y.; Weinell, C.E.; Dam-Johansen, K.; Ring, L.; Kiil, S. Exposure of Hydrocarbon Intumescent Coatings to the UL1709 Heating Curve and Furnace Rheology: Effects of Zinc Borate on Char Properties. *Prog. Org. Coat.* **2019**, *135*, 321–330. [CrossRef]
30. Gravit, M.; Gumenyuk, V.; Sychov, M.; Nedryshkin, O. Estimation of the Pores Dimensions of Intumescent Coatings for Increase the Fire Resistance of Building Structures. *Proc. Procedia Eng.* **2015**, *117*, 119–125. [CrossRef]
31. Geoffroy, L.; Samyn, F.; Jimenez, M.; Bourbigot, S. Intumescent Polymer Metal Laminates for Fire Protection. *Polymer* **2018**, *10*, 995. [CrossRef]
32. Gravit, M.; Ikhiyanov, N.; Radaev, A.; Shabunina, D. Implementation of Elements of the Concept of Lean Construction in the Fire Protection of Steel Structures at Oil and Gas Facilities. *Buildings* **2022**, *12*, 2016. [CrossRef]
33. Piloto, P.A.G.; Balsa, C.; Santos, L.M.C.; Kimura, É.F.A. Effect of the Load Level on the Resistance of Composite Slabs with Steel Decking under Fire Conditions. *J. Fire Sci.* **2020**, *38*, 212–231. [CrossRef]
34. Gravit, M.; Klimin, N.; Karimova, A.; Fedotova, E.; Dmitriev, I. Fire Resistance Evaluation of Tempered Glass in Software ELCUT. *Smart Innov. Syst. Technol.* **2021**, *220*, 523–537. [CrossRef]
35. Gravit, M.; Lavrinenko, M.; Lazarev, Y.; Rozov, A.; Pavlenko, A. Modeling of Cold-Formed Thin-Walled Steel Profile with the MBOR Fire Protection. *Adv. Intell. Syst. Comput.* **2021**, *1259*, 577–592. [CrossRef]
36. Gravit, M.; Shabunina, D. Numerical and Experimental Analysis of Fire Resistance for Steel Structures of Ships and Offshore Platforms. *Fire* **2022**, *5*, 9. [CrossRef]
37. QuickField. Modeling of Two-Dimensional Fields by the Finite Element Method. Available online: https://quickfield.com/ (accessed on 17 December 2022).
38. Schaumann, P.; Tabeling, F.; Weisheim, W. Numerical Simulation of the Heating Behaviour of Steel Profles with Intumescent Coating Adjacent to Trapezoidal Steel Sheets in Fre. *J. Struct. Fire Eng.* **2016**, *7*, 158–167. [CrossRef]
39. Barthelemy, B.; Kruppa, J. *Fire Resistance of Building Structures*; Stroyizdat: Moscow, Russia, 1985; p. 216.
40. Gravit, M.; Shabunina, D.; Antonov, S.; Danilov, A. Thermal Characteristics of Fireproof Plaster Compositions in Exposure to Various Regimes of Fire. *Buildings* **2022**, *12*, 630. [CrossRef]
41. API 2218. Recommended Practices in Petroleum and Petrochemical Processing Plants Structural Fireproofing. Available online: https://www.brindleyengineering.com/wp-content/uploads/2023/01/API-2218-Fireproofing-case-study.pdf (accessed on 3 September 2023).
42. *SP 4.13130.2013*; Systems of Fire Protection. Restriction of Fire Spread at Object of Defense. Requirements to Special Layout and Structural Decisions. Ministry of Emergency of Russia: Moscow, Russia, 2013; 125p. Available online: https://www.admhimki.ru/media/eds/elements/f9f927cb-9929-43ae-be40-fe241849adf0.pdf?ysclid=lmz083d3ki769929025 (accessed on 11 January 2023).
43. *EN 1363-2:1999*; Fire Resistance Tests—Part 2: Alternative and Additional Procedures. British Standards Institution: London, UK, 1999; 16p. Available online: https://nd.gostinfo.ru/document/6239985.aspx (accessed on 2 September 2023).

44. *GOST 53295-2009*; Fire Retardant Compositions for Steel Constructions. General Requirement. Method for Determining Fire Retardant Efficiency. FGU VNIIPO of EMERCOM of Russia: Moscow, Russia, 2010; 14p. Available online: https://technologygroup.ru/images/documents/gost/53295-2009.pdf (accessed on 6 February 2023).
45. *ISO 834-75*; Elements of Building Constructions. Fire-Resistance Test Methods. General Requirements. International Organization for Standardization: New York, NY, USA, 1975; 16p. Available online: https://docs.cntd.ru/document/9055248 (accessed on 2 September 2023).
46. Eurocode 3: Design of Steel Structures—Part 1–2: General Rules Structural Fire Design. Available online: https://www.phd.eng.br/wp-content/uploads/2015/12/en.1993.1.2.2005.pdf (accessed on 21 January 2023).
47. *GOST 8639-82*; Square Steel Pipes. FGUP IPC Publishing House of Standards: Moscow, Russia, 1982; 7p. Available online: https://files.stroyinf.ru/Data/38/3826.pdf?ysclid=lmz0pm3655454170927 (accessed on 4 February 2023).
48. *GOST 57837-2017*; Hot-Rolled Steel I-Beams with Parallel Edges of Flanges. Specifications. JSC SIC Construction: Moscow, Russia, 2017; 44p. Available online: https://docs.cntd.ru/document/1200157342 (accessed on 24 January 2023).
49. Wang, J.X.; Liu, K.; Zhao, C.S.; Wang, Z.L. Research on the Theoretical Calculation Method of Dynamic Response of the Stiffened Plate on the Accommodation of Offshore Platforms under Blast. *Chuan Bo Li Xue/J. Sh. Mech.* **2020**, *24*. [CrossRef]
50. Kim, T.K.; Kim, S.K.; Lee, J.M. Dynamic Response of Drill Floor Considering Propagation of Blast Pressure Subsequent to Blowout. *Appl. Sci.* **2020**, *10*, 8841. [CrossRef]
51. Kung, F.; Yang, M.C. Improvement of the Heat-Dissipating Performance of Powder Coating with Graphene. *Polymers* **2020**, *12*, 1321. [CrossRef]
52. *GOST 27772-2015*; Rolled Products for Structural Steel Constructions. General Specifications. SE UkrSTC Energostal: Kharkov, Ukraine, 2015; 30p. Available online: https://docs.cntd.ru/document/1200133727 (accessed on 4 February 2023).
53. *EN 1991-1-2*; Eurocode 1: Actions on Structures-Part 1–2: General Actions-Actions on Structures Exposed to Fire. European Committee for Standardization: Brussels, Belgium, 2002; 61p. Available online: https://www.phd.eng.br/wp-content/uploads/2015/12/en.1991.1.2.2002.pdf (accessed on 25 August 2023).
54. Markus, E.S.; Snegirev, A.Y.; Kuznetsov, E.A. *Numerical Simulation of a Fire Using Fire Dynamics*; St. Petersburg Polytech-Press: St. Petersburg, Russia, 2021; p. 175.